

Multiphoton ionization and multiphoton resonances in the tunneling regime

R. M. Potvliege

Department of Physics, Durham University, South Road, Durham DH1 3LE, United Kingdom

E. Meşe

*Department of Physics, University of Dicle, Diyarbakır, Turkey and
Department of Chemistry, Durham University, Durham, United Kingdom*

Svetlana Vučić

Institute of Physics, Pregrevica 118, 11080 Belgrade-Zemun, Serbia

(Received 16 February 2010; published 4 May 2010)

The rate of ionization of an atom of helium, argon, or hydrogen exposed to an intense monochromatic laser field and the quasienergy spectrum of their dressed states are studied for values of the Keldysh parameter between 1 and 0.6 and wavelengths between 390 and 1300 nm. The calculations are carried out within the non-Hermitian Floquet theory. Resonances with intermediate excited states significantly affect ionization from the dressed ground state at all the intensities and all the wavelengths considered. The dressed excited states responsible for these structures are large- α_0 states akin to the Kramers-Henneberger states of the high-frequency Floquet theory. Within the single-active-electron approximation, these large- α_0 states become species independent at sufficiently high intensity or sufficiently long wavelength. Apart for the resonance structures arising from multiphoton coupling with excited states, the *ab initio* Floquet ionization rate is in excellent agreement with the predictions of two different calculations in the strong field approximation, one based on a length-gauge formulation of this approximation and one based on a velocity-gauge formulation. The calculations also confirm the validity of the ω^2 expansion as an alternative to the strong field approximation for taking into account the nonadiabaticity of the ionization process in intense low-frequency laser fields.

DOI: [10.1103/PhysRevA.81.053402](https://doi.org/10.1103/PhysRevA.81.053402)

PACS number(s): 32.80.Rm, 42.50.Hz

I. INTRODUCTION

One can broadly distinguish two dynamical regimes of atomic multiphoton processes according to the value of the Keldysh parameter γ_K [1]. For an atom (or ion) of binding energy I_p ,

$$\gamma_K = (2I_p)^{1/2} \omega / F_0 \quad (1)$$

if the field is linearly polarized and can be represented by the electric field vector

$$\mathbf{F} = F_0 \hat{\mathbf{z}} \cos \omega t. \quad (2)$$

(We use atomic units throughout this article, except where specified otherwise.) For $\gamma_K \gg 1$, the interaction of the (classical) light field with the atom is best understood as proceeding through the absorption and stimulated emission of discrete photons, while for $\gamma_K \ll 1$ this interaction can be seen as a perturbation of the atom by a slowly varying quasistatic electric field. The latter regime is often referred to as the “tunneling regime” and the former as the “multiphoton regime.” The distinction between these two cases and the underlying physical picture are grounded in an analysis of multiphoton processes based on the strong field approximation (SFA). This theoretical approach has been immensely successful in predicting and explaining all the main features of a variety of multiphoton processes, in particular high-order above-threshold ionization (HATI) and high-order harmonic generation in strong infrared fields, and the SFA is central to our present understanding of much of the subject [2].

Little is known about the spectrum and the importance of multiphoton resonances between the ground state of the

atom and some of its excited states at the high intensities and long wavelengths characteristic of the tunneling regime. It is often assumed that such resonances play little or no role in these conditions. Indeed, theories based on the SFA are generally in good agreement with experiment in this regime, and these theories postulate that the initial state is coupled only to the continuum by the field [3,4]. It is also often assumed that any resonant excited state would be too broad at the intensities involved for being of any significance. On these premises, the ponderomotive streaking of excited states, which yields series of sharp enhancements of ionization at particular intensities in the multiphoton regime [5,6], should be expected to be insignificant in the tunneling regime. However, it has been known for some time that *ab initio* calculations for long laser pulses may still show clear manifestations of the ponderomotive streaking when $\gamma_K \ll 1$ [7]. In particular, Parker *et al.* found series of resonance enhancements in the rate of ionization of helium at 780-nm wavelength up to the highest intensity they considered, 1.4 PW cm⁻², corresponding to $\gamma_K = 0.4$ [8,9]. These results were calculated by directly solving the time-dependent Schrödinger equation for flat-top pulses, both for the full two-electron problem and for a single-active-electron model. Using the same time-dependent approach in a study the HATI spectrum of helium at 800-nm wavelength, in the single-active-electron approximation, Muller had previously demonstrated that most of the electrons contributing to the recollision plateau are emitted at resonances [10,11]. In these calculations, the enhancements coincided with the mixing of the ground state with unidentified excited states, over narrow ranges of intensity, and they remained prominent up to the highest intensity considered

(0.6 PW cm⁻², corresponding to $\gamma_K = 0.6$). Muller noted that some of the excited states in question have a charge distribution similar to that expected for a Kramers-Henneberger (KH) state—i.e., a bound state supported by the “dressed potential” which determines the dynamics of the electron in high-frequency fields [12].

If we denote by $W(r)$ the potential modeling the interaction of the active electron with the core in the single-active-electron approximation and by \mathbf{r} the position of the electron with respect to the nucleus, the dressed potential is

$$W_{\text{dr}}(\mathbf{r}) = \frac{\omega}{2\pi} \int_{-\pi/\omega}^{\pi/\omega} W(|\mathbf{r} - \alpha_0 \hat{\mathbf{z}} \cos \omega t|) dt \quad (3)$$

for the field defined by Eq. (2). $W_{\text{dr}}(\mathbf{r})$ depends on F_0 and on ω only through the parameter α_0 , which is the excursion amplitude of an electron quivering freely in the field:

$$\alpha_0 = F_0/\omega^2. \quad (4)$$

In the case of atomic hydrogen, $W(r) \equiv -1/r$ and the bound states supported by the corresponding dressed potential are well known [12,13]. In the following we refer to these hydrogen KH states as the Coulomb-KH states. The relevance of $W_{\text{dr}}(\mathbf{r})$ and of α_0 for the ionization dynamics in the infrared comes from the fact that most of the excited states to which the ground state can resonantly couple have a binding energy smaller than the photon energy and therefore behave as predicted by the high-frequency Floquet theory [12] (except when they interact with low-lying states). As the weakly bound states quiver with amplitude α_0 in the rest frame of the nucleus, the long-range Coulomb tail of $W(r)$ dominates the dynamics of the electron when α_0 is sufficiently large. Hence, when α_0 increases the highly excited states of the atom converge to Coulomb-KH states, independently on the species (provided the single-active-electron approximation holds) [14]. The numerical examples given in Ref. [14] and in this article show that the excited spectra of hydrogen, helium, and argon differ greatly for $\alpha_0 < 10$ but are close to each other for $\alpha_0 \gtrsim 15$. Moreover, in the large- α_0 regime, the spectrum of excited states depends on the intensity and on the wavelength of the field primarily through the parameter α_0 . For instance, we show in Sec. III that the spectrum of dressed excited states of argon for a 1300 nm field of 80 TW cm⁻² intensity ($\alpha_0 = 39$) differs little from the corresponding spectrum of helium for a 800-nm field of 500 TW cm⁻² intensity ($\alpha_0 = 37$).

It is worth noting that $\gamma_K < 1$ means that $\alpha_0 \gtrsim 15$ when the wavelength is longer than about 500 nm in the case of He or about 650 nm in the case of Ar (see Fig. 1). Hence, at wavelengths in the infrared, the multiphoton resonances which may play a role in the ionization from the ground state of these species in the tunneling regime are necessarily resonances with large- α_0 states. This article aims at a better understanding of this universal KH spectrum and of its relevance to ionization in long laser pulses.

We tackle the problem within the non-Hermitian Floquet approach, which provides a mathematically rigorous description of the interaction of an atom with a monochromatic laser field based on complex dilation analyticity [15,16]. In this approach, each bound state of the field-free atom turns into a dressed state associated with a complex quasienergy, E , the

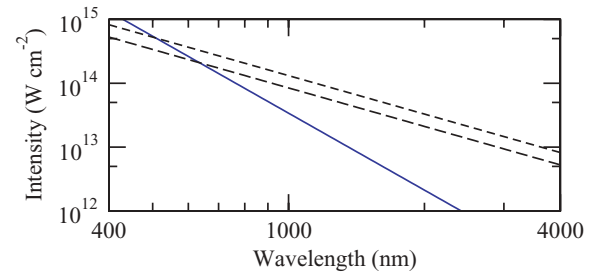


FIG. 1. (Color online) Boundaries of the tunneling regime and of the large- α_0 regime. (Solid line) The intensity above which $\alpha_0 > 15$ a.u. (Short-dashed line) The intensity above which $\gamma_K < 1$ for He. (Long-dashed line) The intensity above which $\gamma_K < 1$ for Ar.

imaginary part of which is related to the rate of ionization from that state, Γ , by $\Gamma = -2 \text{Im } E$. The calculations do not assume the strong-field approximation. They only yield a total rate of ionization (the branching ratios into the different ATI channels cannot be calculated for long-range potentials). However, they make it possible to obtain the whole spectrum of dressed excited states and therefore assign resonance structures to particular intermediate states. Although we do not have access to the ATI spectrum, we can gauge the importance of the resonances by the amplitude of the enhancements and dips they imprint on the rate of ionization from the ground state. We present results for one-electron models of helium and argon, for $\gamma_K \approx 1$ down to $\gamma_K \approx 0.6$. For helium, we consider ionization at either 800-nm or 390-nm wavelengths, in fields of up to 500 TW cm⁻² at 800 nm and 3 PW cm⁻² at 390 nm. The calculations at 390 nm are motivated by results obtained by Parker *et al.* [8] for that particular wavelength. For argon we consider instead ionization in a relatively weak field of 80 TW cm⁻² but for wavelengths ranging from 800 to 1300 nm. We also examine atomic hydrogen at 800 nm for comparison with the helium results.

The Floquet results reported here invite a comparison with the predictions of the SFA. To this effect, we have also calculated the ionization rate within two variants of this approximation, one based on the length-gauge formulation of the theory and one based on the velocity-gauge formulation. Importantly, we use the same single-active-electron model in these calculations as in the full Floquet calculations, so discrepancies between the corresponding rates can be entirely ascribed to inaccuracies inherent to the approximations made in the ionization dynamics in the SFA. The length-gauge formulation is that developed by Perelomov, Popov, and Terent’ev [17,18], modified to converge to an accurate rate in the adiabatic limit. It relies, in effect, on an approximate saddle-point treatment of the time integral defining the ionization amplitude in the SFA. The velocity-gauge formulation is that developed by Faisal [19] and by Reiss [20], and it treats the time integral exactly (this integral is reduced to a generalized Bessel function which can be calculated accurately). We use the correction proposed by Becker *et al.* [21] for taking into account the effect of the Coulomb interaction on the tunneling, which is essential for a quantitative comparison. This correction is not rigorous, but it is known to bring the Faisal-Reiss rate in excellent agreement with benchmark results at much weaker intensities than considered here [21].

We also compare our full Floquet results to the predictions of the ω^2 expansion of Pont *et al.* [22,23]. In this approach, the quasienergy E (and therefore the rate of ionization) is written as a series in powers of the square of the angular frequency of the laser field, namely

$$E = \sum_{n=0}^{\infty} E^{(2n)} \omega^{2n}. \quad (5)$$

The zeroth order term in this expansion is the quasienergy in the adiabatic approximation, E_{ad} . The other terms correct this approximation in a systematic way. This approach does not rely on the SFA and offers an alternative to Keldysh's theory for the treatment of the nonadiabatic corrections. Its mathematical properties are not well understood, however, in particular in what concerns the effect of intermediate-state resonances on the convergence of the expansion. From a numerical point of view, the partial sums of the series have been found to settle to a limit when more and more terms are taken into account, and the convergence is faster at high intensity. For nonresonant ionization of atomic hydrogen by a circularly polarized field, the ω^2 expansion is known to reproduce the Floquet rate well, over a range of intensities and wavelengths [22]. For linear polarization, the only comparison with accurate results made so far has been limited to results in atomic hydrogen for a 616-nm field of intensity up to 3×10^{14} W cm² [23]. Good agreement was found in this case, too, apart for the absence of any resonance structure in the rate obtained by summing the first few terms of the expansion. In Sec. III, we compare the rates of ionization obtained using this approach to the Floquet rates and to those predicted by the SFA to widen the range of systems for which the ω^2 expansion has been tested against other methods.

The different theoretical approaches considered in this article are outlined in Sec. II. The results are presented and discussed in Sec. III. Conclusions are given in Sec. IV.

II. METHOD

A. Floquet calculations

The Floquet calculations presented in this article have been carried out using the same general approach as in Refs. [14,24] and using the same numerical techniques as in Ref. [25]. In a few words, we work within the single-active-electron approximation and represent the interaction of the electron with the core by a model potential $W(r)$, where r is the distance to the nucleus. We also make the dipole approximation, neglect spin-orbit coupling, and assume that the laser field the atom is exposed to can be represented by Eq. (2). The latter assumption makes it possible to seek Floquet solutions of the time-dependent Schrödinger equation for the system, namely solutions of the form

$$|\Psi(t)\rangle = e^{-iEt} \sum_{N=-\infty}^{\infty} e^{-iN\omega t} |\mathcal{F}_N\rangle. \quad (6)$$

The Fourier components $|\mathcal{F}_N\rangle$ satisfy a set of coupled time-independent equations, the ‘‘Floquet equations,’’ which we solve in position space subject to Siegert boundary conditions in the open channels. To this end, we expand the

harmonic components on a basis of spherical harmonics and of complex radial Sturmian functions. We thereby represent the Hamiltonian by a complex matrix. We find the coefficients of the expansion and the quasienergies E by solving the corresponding generalized eigenvalue problem numerically using an Arnoldi algorithm. We eliminate spurious solutions arising from numerical inaccuracies and solutions representing approximate dressed continuum states by retaining only eigen-solutions with quasienergies stable with respect to changes of basis set. This approach is equivalent to diagonalizing the complex-rotated Hamiltonian within the Balslev-Combes theory of resonances [15]. The quasienergies it yields for dressed bound states are complex: for each state, $\text{Im } E = -\Gamma/2$, where Γ is the ionization width of the state. In atomic units, Γ is also the total rate of ionization of the atom when initially in that state. (This rate is thus obtained directly from the quasienergy of the dressed state, and the calculation does not involve an explicit summation of the contributions of the individual ATI channels.)

We assume throughout this work that the laser field is linearly polarized in the z direction. The dressed bound states $|\Psi(t)\rangle$ are therefore eigenvectors of the z component of the orbital angular momentum operator and the field does not couple states of different magnetic quantum numbers m . The dressed bound states are also such that under a reflection about the origin either $|\mathcal{F}_N\rangle \rightarrow (-1)^N |\mathcal{F}_N\rangle$ or $|\mathcal{F}_N\rangle \rightarrow -(-1)^N |\mathcal{F}_N\rangle$ for all values of N . As in Ref. [14], we distinguish these two parity classes by the quantum number σ such that $\sigma = 1$ when $|\mathcal{F}_N\rangle \rightarrow (-1)^N |\mathcal{F}_N\rangle$ and $\sigma = -1$ when $|\mathcal{F}_N\rangle \rightarrow -(-1)^N |\mathcal{F}_N\rangle$.

Equation (6) determines the quasienergies only within an integer multiple of the photon energy. A same dressed state $|\Psi(t)\rangle$ is therefore associated with infinitely many quasienergies of the form $E = E_{\text{ff}} + \Delta_{\text{ac}} + n\hbar\omega$, $n = 0, \pm 1, \pm 2, \dots$, where E_{ff} is the energy of the field-free state and Δ_{ac} is its ac Stark shift. The corresponding solutions of the Floquet equations belong to the same parity class when n is even and to opposite parity classes when n is odd. The complete bound-state quasienergy spectrum is therefore composed of a double infinity of interlacing Brillouin zones, each zone spanning a range of values of $\text{Re } E$ of extension $\hbar\omega$ and repeating itself with period $2\hbar\omega$. For convenience, we fold the real part of the quasienergies into the interval $[-\hbar\omega, 0]$ when plotting their spectrum. Hence, we work in terms of the reduced quasienergy

$$E' = (E \bmod \hbar\omega) - \hbar\omega \quad (7)$$

instead of the quasienergy E defined by Eq. (6). Clearly, $\text{Im } E' \equiv \text{Im } E$. Moreover, there is no difference between E' and E for the dressed states for which $-\hbar\omega \leq \text{Re } E \leq 0$, i.e., for the dressed states from which the atom ionizes by one-photon absorption. Unless forbidden by selection rules, multiphoton resonance occurs between dressed states when the real parts of their reduced quasienergies coincide.

We describe the interaction of the atom with the field in the velocity gauge. In this formulation, the real part of the quasienergies of the dressed highly excited states remains almost constant when the intensity increases, while the real part of the quasienergies of the states for which $I_p \gg \omega$

shifts downward by approximately $-U_p$, where U_p is the ponderomotive energy [6]. One can thus write the ac Stark shift of the dressed ground state in the form

$$\Delta_{\text{ac}} = -U_p + \delta_{\text{np}}, \quad (8)$$

and, except at anticrossings, $|\delta_{\text{np}}| \ll U_p$. Throughout this article we take the dressed ground state to be the dressed state with the largest overlap with the field-free ground state. (This state thus interchanges with the resonant dressed state where their quasienergies anticross each other.)

We present results for atomic hydrogen, argon, and helium. The potential $W(r)$ representing the interaction of the active electron with the core is simply $-1/r$ in the case of hydrogen. For the two complex atoms, we take $W(r)$ to be of the form

$$W(r) = -\frac{1}{r}[1 + Ae^{-\alpha r} + Be^{-\beta r} + Cre^{-\gamma r}]. \quad (9)$$

For argon we take $A = 5.25$, $\alpha = 0.97$, $B = 11.75$, $\beta = 3.7131$, and $C = 0$ [26]. Apart for the deeply bound $1s$, $2s$, $2p$, and $3s$ states supported by this potential, which have no counterpart in the spectrum of the real atom, the field-free energy levels of this model match the centroids of the experimental fine-structure multiplets of the series, converging to the $3p^5 2P_{3/2}^o$ threshold. For helium, we take $\alpha = \gamma = 4$ and $C = 2$ and either $A = 1.23$ and $B = 0$ or $A = 1$, $B = 0.903$, and $\beta = 12$. These two potentials are similar to the static potential of He^+ , which was the model potential adopted in Refs. [10,11]. The two sets of values of A , B , and β are such that for either one the ground-state energy level in the model differs from the exact value by less than 4×10^{-5} a.u. All the He results presented below have been obtained using the model potential for which $A = 1.23$ and $B = 0$. Because the short-range part of the potential plays but a minor role in the dynamical regime we examine in this article, we do not expect significant differences with the results calculated using the model potential for which $A = 1$, $B = 0.903$, and $\beta = 12$; we have verified that this is indeed the case.

B. The ω^2 expansion

Our calculations based on the ω^2 expansion follow Ref. [23]. Thus we express the laser electric field as $\mathbf{F} = F_0 \hat{\mathbf{z}} \cos \tau$, where $\hat{\mathbf{z}}$ is the unit vector in the z direction and $\tau = \omega t$, and we introduce the Hamiltonian

$$H_{\text{dc}}(\tau) = H_0 + F_0 z \cos \tau, \quad (10)$$

where H_0 denotes the Hamiltonian of the model atom in the absence of field. For any value of τ , $H_{\text{dc}}(\tau)$ is effectively the Hamiltonian of the model atom in a static electric field $F_0 \hat{\mathbf{z}} \cos \tau$. We define the state vectors $|\mathcal{F}_{\text{dc}}(\tau)\rangle$ and $|\mathcal{F}_{\text{dc}}^\dagger(\tau)\rangle$ as the eigenvectors of $H_{\text{dc}}(\tau)$ satisfying, respectively, *outgoing* and *ingoing* Siegert boundary conditions and reducing to the field-free ground state in the $F_0 \rightarrow 0$ limit. The corresponding eigenenergies of $H_{\text{dc}}(\tau)$ are respectively the complex dc energy, $E_{\text{dc}}(\tau)$, and its conjugate, $E_{\text{dc}}^*(\tau)$. We calculate these quantities for the same model potentials as in the full Floquet calculations and we use the same numerical methods (i.e., expansion on a complex Sturmian basis in position space and solution of the resulting non-Hermitian generalized eigenvalue

problem). Having $E_{\text{dc}}(\tau)$ makes it possible to calculate the quasienergy in the adiabatic approximation,

$$E_{\text{ad}} = \frac{1}{2\pi} \int_{-\pi}^{\pi} E_{\text{dc}}(\tau) d\tau, \quad (11)$$

and therefore the ionization rate in the adiabatic approximation,

$$\Gamma_{\text{ad}} = -2 \text{Im} E_{\text{ad}}. \quad (12)$$

The coefficients $E^{(2n)}$ of the expansion (5) are obtained from the equation

$$E^{(2n)} = \frac{1}{2\pi} \int_{-\pi}^{\pi} \tilde{E}^{(2n)}(\tau) d\tau, \quad (13)$$

where the functions $\tilde{E}^{(2n)}(\tau)$ are calculated as described in Ref. [23]. In particular,

$$\tilde{E}^{(0)}(\tau) = E_{\text{dc}}(\tau), \quad (14)$$

which implies that $E^{(0)} = E_{\text{ad}}$, and

$$\tilde{E}^{(2)}(\tau) = -\langle \mathcal{F}_{\text{dc}}^\dagger(\tau) | \frac{\partial}{\partial \tau} G_{\text{dc}}(\tau) \frac{\partial}{\partial \tau} | \mathcal{F}_{\text{dc}}(\tau) \rangle. \quad (15)$$

In this last equation,

$$G_{\text{dc}}(\tau) = \frac{Q_{\text{dc}}(\tau)}{E_{\text{dc}}(\tau) - H_{\text{dc}}(\tau)}, \quad (16)$$

with

$$Q_{\text{dc}}(\tau) = 1 - |\mathcal{F}_{\text{dc}}(\tau)\rangle \langle \mathcal{F}_{\text{dc}}^\dagger(\tau)|. \quad (17)$$

Like $\tilde{E}^{(2)}(\tau)$, all the higher-order terms in the expansion (5) can be derived from the dc state vectors $|\mathcal{F}_{\text{dc}}(\tau)\rangle$ and $|\mathcal{F}_{\text{dc}}^\dagger(\tau)\rangle$ and from the dc complex quasienergy $E_{\text{dc}}(\tau)$ [23]. As can be expected given that the interaction potential $F_0 z \cos \omega t$ is invariant for $\omega \rightarrow -\omega$, the expansion (5) does not contain odd-order powers of ω .

The numerical calculation of the coefficients $E^{(n)}$ becomes excessively demanding for $n > 6$, and for this reason we have calculated the partial sums

$$E_m = \sum_{n=0}^m E^{(n)} \omega^{2n} \quad (18)$$

only up to $m = 6$. The corresponding ionization rates, $\Gamma_0 \equiv \Gamma_{\text{ad}}$, Γ_2 , Γ_4 , and Γ_6 , with

$$\Gamma_m = -2 \text{Im} E_m, \quad (19)$$

are discussed in Sec. III.

C. Methods based on the SFA

Rates of ionization calculated within the strong-field approximation are also presented in Sec. III. We consider two formulations of this approximation. In the first one, the calculations are based on the analytical formula for the photoelectron energy spectrum derived by Perelomov, Popov, and Terent'ev [17,18] in their elaboration of Keldysh's original investigation [1]. For ionization from an $(l, m = 0)$ state, the corresponding ionization rate can be written as

$$\Gamma_K(\gamma_K) = (1 + \gamma_K^2)^{3/4} A(\gamma_K) \exp\left[-\frac{2\kappa^3}{3F_0} h(\gamma_K)\right] w_{\text{ad}}, \quad (20)$$

where $\kappa = (2I_p)^{1/2}$,

$$h(\gamma_K) = \frac{3}{2} \frac{1}{\gamma_K} \left[\left(1 + \frac{1}{2\gamma_K^2} \right) \operatorname{arcsinh} \gamma_K - \frac{1}{\beta} \right] - 1 \quad (21)$$

and

$$A(\gamma_K) = \frac{\beta^2}{\sqrt{3\pi}} \sum_{n>[\nu]} \exp[-\alpha(n-\nu)] F_D(\sqrt{\beta(n-\nu)}), \quad (22)$$

with $\beta = 2\gamma_K/(1+\gamma_K^2)^{1/2}$, $\alpha = 2 \operatorname{arcsinh} \gamma_K - \beta$, and

$$\nu = \frac{I_p}{\omega} \left(1 + \frac{1}{2\gamma_K^2} \right) = \frac{1}{\omega} (I_p + U_p). \quad (23)$$

The function $F_D(x)$ is the Dawson integral,

$$F_D(x) = \exp(-x^2) \int_0^x \exp(t^2) dt. \quad (24)$$

It can be shown that $A(\gamma_K) \rightarrow 1$ and that

$$\exp \left[-\frac{2\kappa^3}{3F_0} h(\gamma_K) \right] \sim \exp \left(\frac{2\kappa^3}{3F_0} \frac{1}{10} \gamma_K^2 \right) \quad (25)$$

for $\gamma_K \rightarrow 0$, hence that $\Gamma_K(\gamma_K \rightarrow 0) = w_{\text{ad}}$ [1,17]. In terms of the asymptotic coefficient $C_{\kappa 0}$ in the definition of Ref. [27],

$$w_{\text{ad}} = (2C_{\kappa 0})^2 \left(\frac{6}{\pi} \right)^{1/2} (2l+1) \left(\frac{2\kappa^3}{F_0} \right)^{2n^*-3/2} \times \exp \left(-\frac{2\kappa^3}{3F_0} \right) I_p \quad (26)$$

for detachment of an electron from an atom or a positive ion. Here $n^* = Z/(2I_p)^{1/2}$, Z being the residual charge of the ionic core.

As it is well known [28],

$$w_{\text{ad}} \approx \frac{1}{2\pi} \int_{-\pi}^{\pi} w_{\text{dc}}(|F_0 \cos \tau|) d\tau \quad (27)$$

for $F_0/\kappa^3 \ll 1$, where $w_{\text{dc}}(F)$ is the WKB rate of ionization by a static electric field of strength F [29]:

$$w_{\text{dc}}(F) = (2C_{\kappa 0})^2 (2l+1) \left(\frac{2\kappa^3}{F} \right)^{2n^*-1} \exp \left(-\frac{2\kappa^3}{3F} \right) I_p. \quad (28)$$

The ionization rate w_{ad} is thus a weak-field approximation of the adiabatic rate Γ_{ad} defined by Eq. (12). We can therefore expect that replacing w_{ad} by Γ_{ad} in Eq. (20) would improve the accuracy of the calculation. We refer to the resulting ionization rate,

$$\Gamma_{\text{MK}}(\gamma_K) = (1 + \gamma_K^2)^{3/4} A(\gamma_K) \exp \left[-\frac{2\kappa^3}{3F_0} h(\gamma_K) \right] \Gamma_{\text{ad}}, \quad (29)$$

as the modified Keldysh rate. For $\kappa^3/F_0 \gg 1$, $\Gamma_K(\gamma_K) \approx \mathcal{C}(\gamma_K)w_{\text{ad}}$, and $\Gamma_{\text{MK}}(\gamma_K) \approx \mathcal{C}(\gamma_K)\Gamma_{\text{ad}}$ when $\gamma_K \ll 1$, where

$$\mathcal{C}(\gamma_K) = \exp \left(\frac{2\kappa^3}{3F_0} \frac{1}{10} \gamma_K^2 \right). \quad (30)$$

We also present results obtained within Faisal's and Reiss's velocity-gauge formulation of the SFA [19,20], corrected

for the Coulomb interaction between the photoelectron and the ionic core as proposed by Becker *et al.* [21]. In the single-active-electron approximation, the corresponding Coulomb-corrected Faisal-Reiss rate for ionization from an S state by the linearly polarized field (2) is [30]

$$\Gamma_{\text{CCFR}} = 2\pi C^2 \sum_{n>[\nu]} \int (U_p - n\omega)^2 J_n^2 \left(\alpha_0 \mathbf{k}_n \cdot \hat{\mathbf{z}}; \frac{U_p}{2\omega} \right) \times |\langle \chi(\mathbf{k}_n) | \phi_i \rangle|^2 |\mathbf{k}_n| d\mathbf{k}_n. \quad (31)$$

In this equation, $|\mathbf{k}|_n = [2(n\omega - I_p - U_p)]^{1/2}$, the function $J_n(a, b)$ is the generalized Bessel function,

$$J_n(a; b) = \sum_{p=-\infty}^{\infty} J_{n+2p}(a) J_p(b), \quad (32)$$

$|\phi_i\rangle$ denotes the state vector of the field-free initial state, and $|\chi(\mathbf{k}_n)\rangle$ is the field-free plane wave of wave vector \mathbf{k}_n in the normalization where $\langle \chi(\mathbf{k}) | \chi(\mathbf{k}') \rangle = \delta(\mathbf{k}' - \mathbf{k})$. The Coulomb correction is effected by the factor C^2 : $C^2 = 1$ for detachment from a short-range potential while $C^2 = (\kappa^3/F_0)^{2n^*}$ for ionization of an atom [21]. We evaluate the quantity $\langle \chi(\mathbf{k}_n) | \phi_i \rangle$ by Fourier transforming the wave function of the field-free initial state calculated using the model potentials and the basis set method described in Sec. II A. Depending on its arguments, we calculate the generalized Bessel function either by direct summation or by using accurate asymptotics [31].

III. RESULTS AND DISCUSSION

A. The SFA and the ω^2 expansion

We start by comparing the predictions of the ω^2 expansion to those of calculations based on the strong-field approximation. The rate of ionization from the ground state of He is shown in Fig. 2 for two different wavelengths, 390 nm (blue curves) and 800 nm (orange curves), and for intensities up to $2 \times 10^{15} \text{ W cm}^{-2}$. The Coulomb-corrected Faisal-Reiss rate Γ_{CCFR} , defined by Eq. (31), is given for both wavelengths. The modified Keldysh rate Γ_{MK} , defined by Eq. (29), is shown only for 390 nm. In these two variants of the SFA, the rate of ionization has a minimum at each multiphoton threshold, i.e., at each intensity at which an ATI channel closes. These channel closures occur at intensities separated by 0.22 PW cm^{-2} at 390 nm and by 0.026 PW cm^{-2} at 800 nm (the difference arises from the faster variation of U_p at 800 nm). The drop at the threshold is smaller at the longer wavelength, too, since at a same intensity fewer ATI channels contribute to the total rate at 390 nm than at 800 nm. The modified Keldysh rate varies more smoothly than the Coulomb-corrected Faisal-Reiss rate between thresholds. The complicated variation of the latter is primarily due to the oscillations of the generalized Bessel functions appearing in Eq. (31), not to multiphoton resonances [32]. There is no such oscillations in the modified Keldysh rate. However, apart for these fine details, the Coulomb-corrected Faisal-Reiss rate and the modified Keldysh rate are in close agreement with each other, both at 390 nm and at 800 nm. The agreement shows that the choice of gauge is not critical in this problem and confirms the validity of the Coulomb correction proposed in Ref. [21].

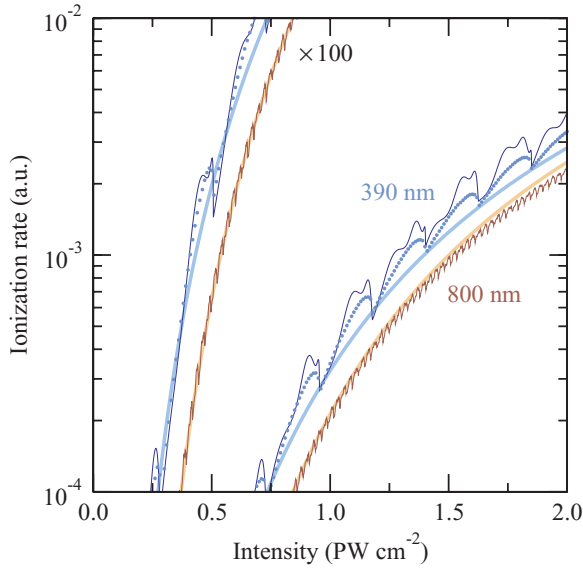


FIG. 2. (Color online) The rate of ionization from the ground state of He vs. intensity in three different approximations. The rate is multiplied by a factor of 100 where lower than 1×10^{-4} a.u. (Thin solid curves) Rate predicted by the Coulomb-corrected Faisal-Reiss approximation, Γ_{CCFR} . (Thick solid curves) Rate calculated by summing the ω^2 expansion up to order ω^6 , Γ_6 . Results are shown for 390-nm wavelength (upper curves) and for 800-nm wavelength (lower curves). The blue circles represent the modified Keldysh rate, Γ_K (390 nm only).

In contrast to the SFA, the ω^2 expansion yields rates varying smoothly at thresholds. In the range of intensities spanned by the figure, the expansion converges rapidly at 800 nm. The speed at which the expansion converges increases with intensity and, for a same intensity, is slower at 390 nm than at 800 nm (see Table I) [33]. However, it is fast enough even at 390 nm that above 0.3 PW cm^{-2} the rate obtained by summing the expansion up to order ω^6 , Γ_6 , can be considered to be converged for any practical purpose. Higher-order terms are likely to be important at weaker intensities at 390 nm, as shown by the large difference between the values of Γ_4 and Γ_6 at 0.2 PW cm^{-2} for that wavelength.

Also noteworthy is the agreement between the predictions of the SFA and of the ω^2 expansion in regards to the overall

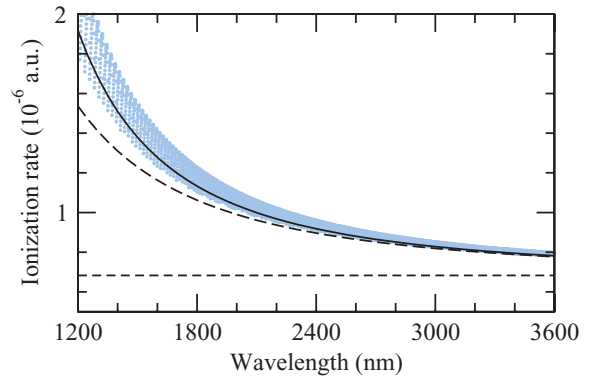


FIG. 3. (Color online) The rate of ionization from the dressed ground state of argon at an intensity of 80 TW cm^{-2} vs. the wavelength of the field. (Short-dashed line) Adiabatic rate, Γ_{ad} . (Long-dashed and solid curves) Results obtained by summing the ω^2 expansion up to order ω^2 and up to order ω^6 , respectively. (Blue circles) Modified Keldysh rate.

magnitude of the rate (see Fig. 2). These two approaches are particularly close at low intensity. The agreement gradually deteriorates as the intensities increases above 1.5 PW cm^{-2} , which is the critical intensity for over-the-barrier ionization.

The two approaches are also compared in Fig. 3 for the case of ionization from the ground state of argon by a strong midinfrared laser field. As in Ref. [34], the intensity is set at $8 \times 10^{13} \text{ W cm}^{-2}$ and the wavelength varies up to 3600 nm. Again, one can note the close agreement between the SFA and the ω^2 expansion and the rapidity with which the latter converges at the longest wavelength (compare Γ_6 to Γ_2 and Γ_0).

The convergence of the SFA and of the ω^2 expansion to the adiabatic rate as the wavelength increases is also in line with Keldysh's analysis of the decrease in importance of the nonadiabatic effects for decreasing values of γ_K [1]. In Fig. 3, $\gamma_K = 0.29$ at 3600 nm. If one takes only the most important nonadiabatic correction to the adiabatic rate into account, namely, since $\kappa^3/F_0 \gg 1$, the factor $\mathcal{C}(\gamma_K)$ defined by Eq. (30), the Keldysh theory predicts that the ionization rate for the 3600 nm field should be 16% larger than in the adiabatic approximation. Almost exactly the same result is obtained from the ω^2 expansion: at this wavelength, Γ_6 is 15% larger

TABLE I. The rate of ionization from the ground state of He, in a.u., as obtained by summing the ω^2 expansion to zeroth, second, fourth, and sixth order in ω at four different intensities. The numbers between brackets indicate the powers of 10.

I	Γ_0	Γ_2	Γ_4	Γ_6
Wavelength: 390 nm				
0.2 PW cm^{-2}	1.69(−9)	1.79(−8)	7.33(−8)	1.53(−7)
0.3	8.27(−8)	5.11(−7)	1.24(−6)	1.66(−6)
0.5	3.96(−6)	1.34(−5)	1.94(−5)	1.96(−5)
1.0	1.80(−4)	3.17(−4)	3.27(−4)	3.25(−4)
Wavelength: 800 nm				
0.2 PW cm^{-2}	1.69(−9)	5.53(−9)	8.67(−9)	9.74(−9)
0.3	8.27(−8)	1.85(−7)	2.26(−7)	2.31(−7)
0.5	3.96(−6)	6.20(−6)	6.54(−6)	6.54(−6)
1.0	1.80(−4)	2.13(−4)	2.13(−4)	2.13(−4)

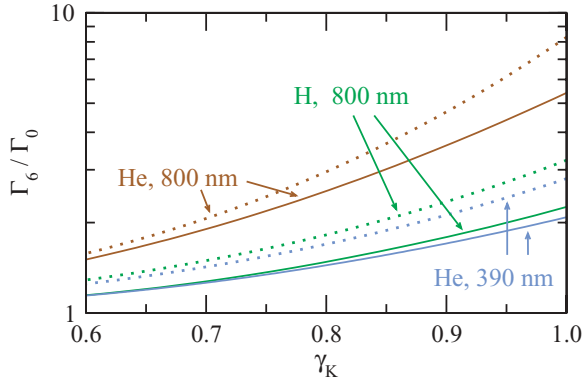


FIG. 4. (Color online) The ratio of the ionization rate predicted by the ω^2 expansion, Γ_6 , to the adiabatic ionization rate, $\Gamma_0 \equiv \Gamma_{\text{ad}}$, for ionization from the ground state of helium in strong laser fields of 390 nm or 800 nm wavelength, and for ionization from the ground state of atomic hydrogen at 800 nm. The dotted curves show the corresponding results in the Keldysh theory taking into account only the leading nonadiabatic correction to Γ_{ad} , namely the factor $\mathcal{C}(\gamma_K)$ defined by Eq. (30).

than Γ_{ad} . There is also a good agreement between the SFA and the ω^2 expansion on the magnitude of the nonadiabatic corrections at the shorter wavelengths and stronger fields considered in Fig. 2, although the factor $\mathcal{C}(\gamma_K)$ significantly overestimates these corrections when $\gamma_K \approx 1$ (see Fig. 4). We

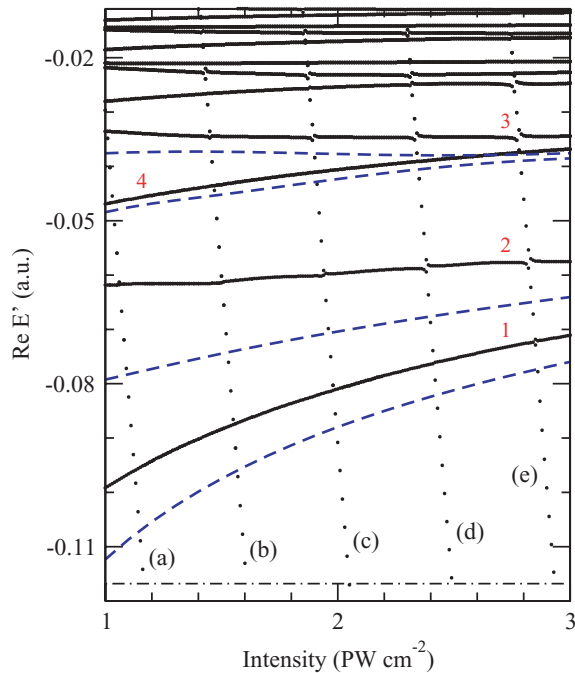


FIG. 5. (Color online) The $(\sigma = 1, m = 0)$ quasienergy spectrum of helium at 390-nm wavelength. The dressed ground state sweeps through resonance with the $(\sigma = 1, m = 0)$ dressed excited states five times in the range of intensities spanned by the figure; the letters (a) to (e) identify the corresponding sequences of crossings. No results are shown below the dash-dotted line, which indicates the $\text{Re } E = -\hbar\omega$ threshold. (Dashed curves) The energies of the four lowest σ_g Coulomb-KH states [13]. The numbers are labels identifying Floquet states for reference in the text.

surmise from these results that the ω^2 expansion, truncated to its first few terms, corrects the adiabatic quasienergy only for the nonadiabatic nature of the tunneling stage of ionization in an oscillating field, and not for the presence of multiphoton resonances and of multiphoton thresholds.

B. Multiphoton resonances in intense fields

1. Quasienergy spectrum

As noted in Sec. II, the solutions of the Floquet equations divide into symmetry classes identified by the parity quantum number σ and (for linear polarization) the magnetic quantum number m . A large section of the $(\sigma = 1, m = 0)$ quasienergy spectrum of He at a wavelength of 390 nm is shown in Fig. 5 for intensities between 1×10^{15} and 3×10^{15} W cm^{-2} . The corresponding results for a wavelength of 800 nm and intensities between 1×10^{14} and 5×10^{14} W cm^{-2} are shown in Fig. 6. The spectrum of atomic hydrogen is also shown in Fig. 6. In both figures, each dot represents the real part of a calculated quasienergy folded into the interval $[-\hbar\omega, 0]$, as defined by Eq. (7). An infinity of dressed Rydberg states accumulate under the ionization threshold, i.e., at $\text{Re } E$ just below 0, and consequently this region is omitted from the diagrams.

The real part of the quasienergy of the dressed ground state varies (almost) linearly with intensity. It shifts downward with respect to the continuum threshold. Its trajectory can be traced by the oblique rectilinear alignments of data points streaking the spectrum periodically. The dressed excited states it may interact with swap between the $(\sigma = 1, m = 0)$ symmetry and the $(\sigma = -1, m = 0)$ symmetry at each crossing of a multiphoton threshold. Accordingly, in Figs. 5 and 6 the dressed ground state is shown only in the intervals of intensity where it becomes resonant with the $(\sigma = 1, m = 0)$ states. The

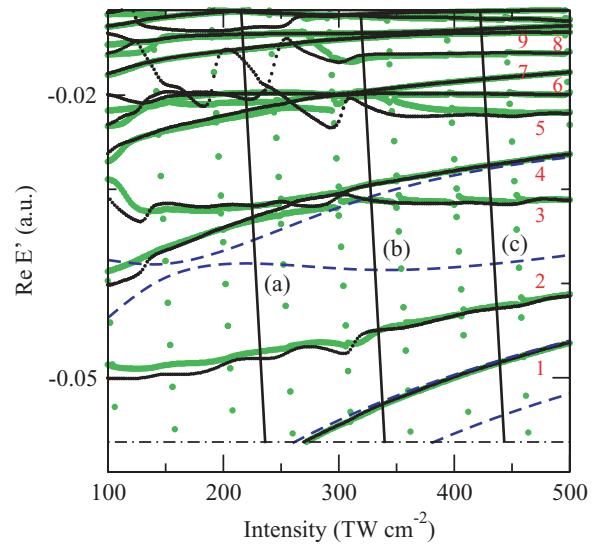


FIG. 6. (Color online) As in Fig. 5 but for a wavelength of 800 nm. The $(\sigma = 1, m = 0)$ quasienergy spectrum of hydrogen is also shown (large green dots). Three of the eight sequences of crossings the dressed ground state of He has with the $(\sigma = 1, m = 0)$ dressed excited states between 100 and 500 TW cm^{-2} are shown and are identified by the labels (a) to (c); for clarity, the other five sequences of crossings are not represented.

resonances occur where the curves described by the real part of the quasienergies of the dressed excited states cross that described by the real part of the quasienergy of the dressed ground state (within an integer multiple of the photon energy). These crossings are direct (i.e., they are not avoided) in the spectrum of helium shown in Fig. 6. However, a number of avoided crossings involving the dressed ground state are visible in the spectrum of hydrogen shown in the same diagram as well as in the spectrum of helium shown in Fig. 5.

All the dressed excited states found in this work can ionize by absorption of a single photon, both at 390 nm and at 800 nm. The predictions of the high-frequency Floquet theory are thus relevant as far as these states are concerned. In particular, and as long as the single-active-electron approximation holds, one should expect (1) that the quasienergy levels depend primarily on the excursion amplitude $\alpha_0 = F_0/\omega^2$, and consequently that fields of different intensities and wavelengths but same values of α_0 give rise to similar excited quasienergy spectra; and (2) that these spectra should be close to the bound state spectrum of the dressed potential $W_{\text{dr}}(\mathbf{r})$. The parameter α_0 varies between 12 and 21 a.u. in the range of intensity spanned by Fig. 5 and between 16 and 37 a.u. in that spanned by Fig. 6. Since for $\alpha_0 \gg 0$ a loosely bound electron has little probability to be in the region of space where the short-range part of the atomic potential is significant, the spectrum of dressed excited states becomes species independent at sufficiently high intensities [14]. The similarity between the excited spectra of helium and atomic hydrogen shown in Fig. 6 is an example of this general trend. (Significant discrepancies can be noticed near 100 TW cm⁻², but, except at avoided crossings with the dressed ground state, the two spectra are almost identical above 350 TW cm⁻².)

At the intensities considered, α_0 is also sufficiently large that the general structure of the spectrum is the same in Figs. 5 and 6. One can distinguish three interlaced Rydberg series of dressed excited states, namely a series of states that shift smoothly upward (e.g., the states labeled 1, 4, and 7 in Fig. 6), a series of states that shift less overall but have rapid variations over narrow ranges of intensity (e.g., States 2, 3, 5, and 8), and, starting at $\text{Re } E' \approx -0.02$ a.u. at 800 nm (above 300 TW cm⁻²), another series of states that shift little with respect to the continuum threshold (e.g., States 6 and 9). In Figs. 5 and 6, and throughout the rest of this article, the states are labeled according to their large α_0 limit, not their zero-field limit, and in the same way at all wavelengths. For example, State 3 in Fig. 5 maps to State 3 in Fig. 6 if the wavelength is changed from 390 nm to 800 nm and similarly for the other states. As we will see below, at 800 nm States 2, 3, 5, and 8 have a larger ionization width than most of the other dressed excited states in this region of the spectrum (with the exception of State 1). It has been observed in calculations on other species that states with a large ionization width can interact with even broader dressed states and as a result shift rapidly in narrow intervals of intensity [14]. Such interactions with states not shown in Fig. 6 may thus explain the complicated behavior of the quasienergy of States 2, 3, 5, and 8. (While we are confident to have found all the dressed excited states with an ionization width smaller than 0.01 a.u., it is possible that broader states are also present—e.g., the dressed $2s$ and $2p$ states and, possibly, light-induced states [14].)

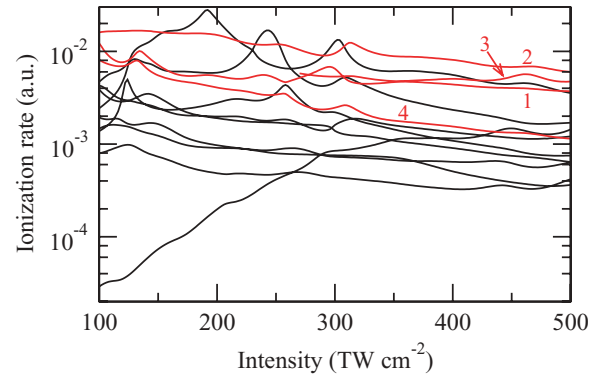


FIG. 7. (Color online) The rates of ionization from the dressed excited states of He shown in Fig. 6. The red curves are the rates for States 1–4.

Given their symmetry, the dressed excited states shown in Figs. 5 and 6 should converge in quasienergy to the σ_g Coulomb-KH states (in the terminology of Ref. [13]). The four lowest of the latter are represented by dashed curves in these two diagrams. The quasienergy curves which have these four Coulomb-KH curves for the high-frequency limit are those of States 1, 2, 3, and 4. As should be expected, these four dressed states are closer to the four Coulomb-KH states at 390 nm (Fig. 5) than at 800 nm (Fig. 6). That State 1 coincides with the second lowest Coulomb-KH state in Fig. 6 is an accident: this is State 2, not State 1, which converges to the second lowest Coulomb-KH state in the high-frequency limit.

Our results are also consistent with the prediction of the high-frequency Floquet theory that the dressed states for which $-\hbar\omega < \text{Re } E < 0$ become stable against ionization in the large α_0 limit [12]. This strong-field stabilization here manifests by an overall decrease in the rate of ionization from the dressed excited states, as is clearly shown by Fig. 7. For instance, the rate of ionization from State 4 decreases by a factor 7 between 100 and 500 TW cm⁻². However, stabilization is not monotonical and is not as rapid for all the states. In particular, for States 2, 3, 5, and 8 ionization is significantly enhanced in certain intervals of intensity. The enhancements coincide with the intermittent, rapid variation of the real part of their quasienergy mentioned above. The dressed $7i_{m=0}$ state differs from the other dressed states represented in Fig. 7 in having an ionization rate which is markedly lower in weak fields (3×10^{-5} a.u. at 100 TW cm⁻²) and which increases (almost) monotonically between 100 and 500 TW cm⁻². The low rate of ionization in weak fields is expected for states of large orbital angular momentum, as those states are not strongly coupled to the continuum. Whether this particular dressed state would not stabilize in sufficiently strong fields, in violation of the general prediction of the high-frequency Floquet theory, cannot be ascertained from our numerical results; however, it is likely that it eventually would, since it mixes with other bound states and loses its identity as the intensity increases. It has been observed that the intensity at which stabilization sets in tends to increase with the angular momentum of the state [35], and the absence of a sustained decrease in the rate of ionization from the dressed $7i_{m=0}$ state in Fig. 7 may mean that this state reaches the stabilization regime only above 500 TW cm⁻² at 800 nm.

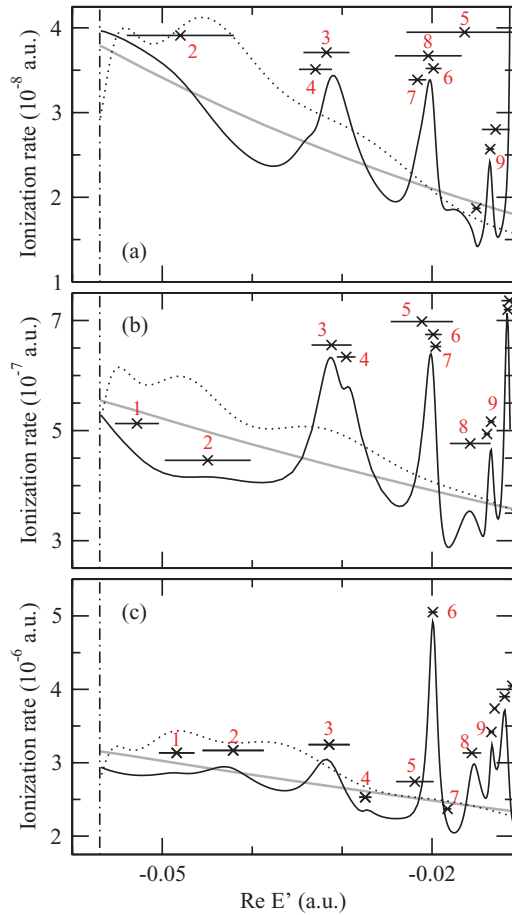


FIG. 8. (Color online) The rate of ionization from the dressed ground state of He over the three ranges of intensities for which this state is shown in Fig. 6, vs. the real part of its quasienergy. The wavelength is 800 nm. (Solid black curves) Full Floquet calculation. (Dotted curves) Coulomb-corrected Faisal-Reiss theory. (Solid gray curves) Results obtained by summing the ω^2 expansion up to order ω^6 . The crosses indicate the positions of the resonances and the horizontal bars the ionization widths of the corresponding dressed excited states at their crossing with the dressed ground state. (The vertical positions of these markers are arbitrary.) The numbers identify the states as per Fig. 6.

2. Ionization rate

The rate of ionization from the dressed ground state of He at 800 nm wavelength is shown in Fig. 8, for the sequences of crossings identified by the letters (a), (b), and (c) in Fig. 6. To facilitate the comparison, the ionization rate is plotted as a function of the real part of the ground-state quasienergy (with the latter folded into the interval $[-\hbar\omega, 0]$). The intensity thus increases from right to left. It varies from 215 to 236 TW cm^{-2} in Fig. 6(a), from 319 to 340 TW cm^{-2} in Fig. 6(b), and from 422 to 443 TW cm^{-2} in Fig. 6(c), which correspond to values of the Keldysh parameter γ_K of about 0.95, 0.79, and 0.69, respectively. The number of photons the atom must absorb to be ionized from the dressed ground state is 25 in Fig. 6(a), 29 in Fig. 6(b), and 33 in Fig. 6(c).

A number of resonance enhancements of the ionization rate are visible in these diagrams. To make it easier to correlate these enhancements with the quasienergy spectrum, a cross is plotted at each value of $\text{Re}E'$ at which the dressed ground

state is resonant with a dressed excited state in Fig. 6. For each resonance, the ionization width of the latter, Γ_{exc} , is indicated by an horizontal bar of length Γ_{exc} centered on the cross. We see that most crossings are associated with a discernible structure in the rate, sometimes a modest enhancement or a shoulder, sometimes a prominent peak. In all cases where a structure is associated with a single crossing, the width of this structure matches the ionization width of the corresponding excited state. (For the crossings covered by the figure, the resonant excited states are all much broader than the ground state. If the opposite was the case, we would instead expect that the width of the resonance structure matches the width of the ground state.) The general reduction in the widths of the excited states as the intensity increases comes out clearly if one compares the three panels. One can also notice similarities in the way states belonging to a same series of dressed excited states affect ionization from the ground state: States 6 and 9 are both associated with sharp enhancements while States 1, 4, and 7 are not associated with any visible resonance structures or only with minor enhancement. We surmise from this that states from the latter series are more weakly coupled to the ground state by the field than those of the series States 6 and 9 belong to.

While the absolute magnitude of the enhancements increases from Fig. 8(a) to Fig. 8(c), their relative magnitude tends to decrease. The difference is marked for the enhancement associated with State 3. However, even at the intensities considered in (c) ($\gamma_K \approx 0.69$), the resonances with the states crossed at $\text{Re}E' \approx -0.015$ a.u. still enhance the rate by about 50% while that with State 6 enhances the rate by a factor of 2.

We also compare, in Fig. 8, the exact Floquet ionization rate to the predictions of the strong-field approximation (in the Coulomb-corrected Faisal-Reiss formulation) and of the ω^2 expansion. As noted in Sec. III A, at the intensities and wavelength considered, Γ_6 (represented by the thick gray curves in the diagram) may be taken to be representative of the predictions of this theory. The predictions of the Coulomb-corrected SFA are similar to those of the ω^2 expansion, with the former giving slightly larger rates (except immediately above the multiphoton thresholds, where in the SFA the ionization rate drops owing to closure of the lowest ATI channel). As found at lower intensities [21,23], both the ω^2 expansion and the Coulomb-corrected SFA yield ionization rates in good general agreement with the exact Floquet rates. However, they are larger than the “baseline” of the resonance peaks modulating the latter. We also note that, contrary to the predictions of SFA, the enhancements of ionization found in the Floquet calculations are all correlated with resonances with intermediate excited states.

Although hydrogen and helium have similar spectra of quasienergies when α_0 is large, the way in which the rate of ionization from the ground state is affected by the resonances with the dressed excited states differs between these two species. To establish this, we show, in Fig. 9, how the hydrogen rate varies between 100 TW cm^{-2} ($\gamma_K = 1.1$) and 300 TW cm^{-2} ($\gamma_K = 0.62$). The wavelength is 800 nm. The calculation could not resolve the accumulation of crossings with dressed Rydberg states at intensities immediately above those at which the dressed ground state passes a multiphoton threshold. These regions are shaded in the figure. Where

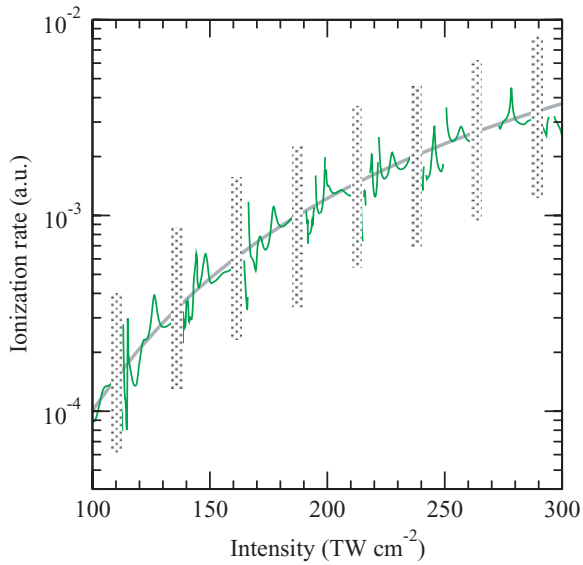


FIG. 9. (Color online) The rate of ionization from the ground state of atomic hydrogen at 800-nm wavelength. (Green curve) Results of the Floquet calculation. (Thick gray curve) Results obtained by summing the ω^2 expansion up to order ω^6 [23]. The shaded regions cover the regions in which unresolved dressed Rydberg states accumulate.

calculated, the rate shows a number of strong resonance features originating from the interaction of the ground state with moderately excited states. Hydrogen having a smaller binding energy, its rate of ionization is larger than that of helium. They differ by five orders of magnitude at 200 TW cm^{-2} for that wavelength, which means that the width of the dressed ground state is comparable to or exceeds the widths of most of the resonant dressed excited states. Consequently, a number of their crossings with the dressed ground state are avoided, not direct. In Fig. 9, these avoided crossings result in discontinuities in the ionization rate and gaps at intensities where the dressed ground state cannot be identified. They can be seen in the hydrogen spectrum of Fig. 6 even at intensities as high as 460 TW cm^{-2} ($\gamma_K = 0.50$). We also note from Fig. 9 that at the highest intensities resonances with the more highly excited states tend to suppress ionization rather than increase it. This reduction is not surprising since in such strong fields many of these excited states are more stable against ionization than the ground state. For example, at around 290 TW cm^{-2} , the ground state is resonantly coupled to the dressed $6s$ state by 20-photon absorption. Immediately outside the crossing the ionization rate from the $6s$ state is only a quarter of that from the ground state, with the consequence that at the very crossing, where the two states mix strongly, the ground-state rate is reduced.

The ionization rate predicted by the ω^2 expansion, Γ_6 , is also represented in Fig. 9. As for helium at the same wavelength, this approximation reproduces the exact Floquet rate well, apart for the absence of enhancements and drops where the ground dressed state interacts with excited states.

We now come back to ionization from the ground state of helium at 390 nm. This system is of particular interest in the context of the present work because the time-dependent calculations of Ref. [8] indicate a marked reduction of the

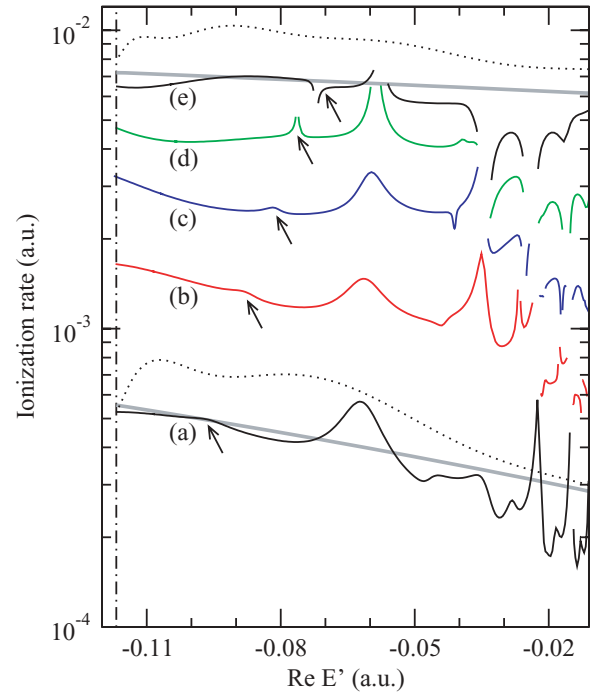


FIG. 10. (Color online) The rate of ionization from the dressed ground state of He over the five sequences of crossings labeled (a) to (e) in Fig. 5, vs. the real part of its quasienergy. The wavelength is 390 nm. (Dotted curves) Coulomb-corrected Faisal-Reiss theory. (Thick solid gray curves) Results obtained by summing the ω^2 expansion up to order ω^6 . The other curves show the results of the full Floquet calculation. The Floquet results are discontinuous at avoided crossings with dressed excited states. The arrows indicate the resonance structures associated with the crossings between the dressed ground state and State 1.

amplitude of the resonance structures above 2 PW cm^{-2} . We show the Floquet rate of ionization in Fig. 10, for the five series of crossings visible in Fig. 5. From Figs. 10(a) to 10(e), the Keldysh parameter varies from around 0.93 to around 0.56, and the number of photons the atom must absorb to be ionized increases from 13 to 21. The rate of ionization from the ground state is about the same as in Fig. 9 (i.e., it is three or four orders of magnitude larger here than in Fig. 6), with the same consequence that many of its crossings with dressed excited states are avoided. In Fig. 10(a), resonances with excited states normally enhance ionization and, close to the threshold, give rise to sharp Fano profiles. This variation is typical of the multiphoton regime for the case where the ground state has a smaller ionization width than most or all the excited states it interacts with. The picture changes gradually as the intensity increases, and in Fig. 10(e) we mostly find avoided crossings and a reduction of ionization at the resonances, not an enhancement. Also, the widths of the resonance structure becomes dominated by the width of the ground state rather than the widths of the excited states, as the former increases with intensity while the latter generally decrease. The change in the resonance structure associated with the crossing with State 1 is an example of the general trend: going from Fig. 10(a) to Fig. 10(e), the resonance first produces a sharper and sharper enhancement of ionization, and then an avoided crossing and a reduction of ionization.

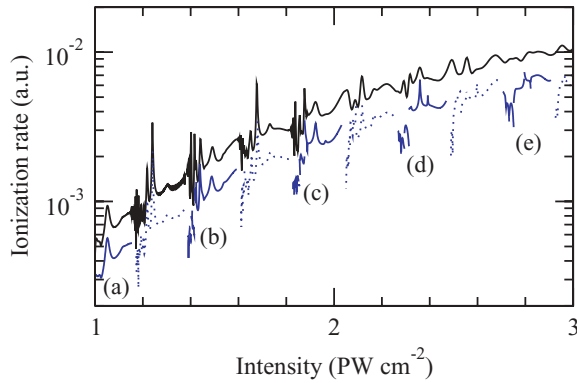


FIG. 11. (Color online) The rate of ionization from the ground state of He at 390-nm wavelength as a function of the intensity. (Solid black curve) Results of the time-dependent calculations of Ref. [8]. (Blue curves) Present results, rescaled in intensity as described in the text. The Floquet rate is represented by a solid curve in the range of intensity where the dressed ground state sweeps through resonance with dressed excited states of $(\sigma = 1, m = 0)$ symmetry and by a dotted curve in between. The labels (a) to (e) refer to the sequences of crossings shown in Fig. 5.

As in Fig. 9, the ionization rate predicted by the ω^2 expansion is in good overall agreement with the exact Floquet rate, except where resonances dominate the latter. The SFA tends to overestimate the ionization rate but rarely by more than 50%. The agreement of the Coulomb-corrected Faisal-Reiss rate with the exact Floquet rate is as good in Fig. 10(e) as in Fig. 10(a), although in Fig. 10(e) the intensity of the field (about 2.8 PW cm^{-2}) is almost twice the critical intensity for over-the-barrier ionization (1.5 PW cm^{-2}).

Finally, we compare the rate of ionization of helium shown in Fig. 10 to the results of Parker *et al.* [8]. These authors calculated the ionization rate by solving the full two-electron time-dependent Schrödinger equation *ab initio*, for a flat-top pulse, at 60 different intensities ranging from almost 0 to 3.4 PW cm^{-2} . The rate was then obtained at intermediate intensities using a one-electron model of the atom, the parameters of this model being chosen so that the one-electron calculations reproduced the two-electron results at the intensities where the latter were available. The resulting time-dependent rates are compared to the Floquet rates in Fig. 11 for intensities ranging from 1 to 3 PW cm^{-2} . The dressed excited states the dressed ground state is resonant with alternate between the $(\sigma = 1, m = 0)$ symmetry and the $(\sigma = -1, m = 0)$ symmetry as the intensity increases. The Floquet rate is indicated by a dotted curve in the intensity regions in which $\sigma = -1$. In the range of intensities spanned by the figure, the regions in which $\sigma = 1$ are the same as those for which the rate is shown in Fig. 10. (The rate is plotted as a function of $\text{Re}E'$ in Fig. 10 and as a function of intensity in Fig. 11.) The Floquet rate is discontinuous at avoided crossings and is not calculated where the dressed ground state encounters closely spaced dressed Rydberg states.

The intensities at which multiphoton resonances occur depend on the nonponderomotive part of the ac Stark shift of the ground state with respect to the continuum threshold—i.e., the quantity δ_{np} defined by Eq. (8)—although at 390 nm this nonponderomotive contribution accounts for less than 1% of the total shift. We infer from Ref. [9] that δ_{np} is a factor

1.8 larger in the model used in these calculations than in the present work. This difference can be compensated by multiplying the intensity by a constant scaling factor when plotting the Floquet results, since both δ_{np} and the total ac Stark shift are approximately proportional to the intensity. The correction amounts to a reduction of the intensity by 0.93%. As can be seen from Fig. 11, the agreement between the two calculations on the positions of the resonance enhancements is excellent when this scaling is applied, despite the differences in the underlying models. The Floquet rate is smaller than the time-dependent rate by a constant factor close to 1.6; however, the difference would be less if we were to multiply the former by a factor of 2 to account for the presence of two equivalent electrons in the ground state of the atom. A more significant discrepancy between the two sets of results is that the rate of ionization predicted by the time-dependent calculation does not dip in the same way as the Floquet rate where the ground state sweeps through resonance with highly excited states. This discrepancy may arise from the population of dressed excited states during the turn-on of the field in the time-dependent calculations: if there is a significant admixture of dressed excited states decaying more rapidly than the dressed ground state in the wave function, which is not unlikely in the regions of avoided crossings, the decay of the population in the vicinity of the nucleus may reflect ionization from these excited states more than ionization from the ground state. Since the ground state is deduced from this decay, the dips at the resonances with Rydberg states may be masked. However, further work on the relationship between the two approaches would be useful in order to elucidate the origin of this discrepancy.

We conclude from Figs. 10 and 11 that the reduction in the amplitude of the resonance enhancements above 2 PW cm^{-2} found in the time-dependent calculations [8] is not due to a reduction in the interaction of the dressed ground state with dressed excited states. To the contrary, it is clear from the Floquet results that such resonances can still be expected to affect ionization from the ground state significantly at intensities well above 2.5 PW cm^{-2} .

C. Multiphoton resonances in strong midinfrared fields

Turning to longer wavelengths, we now focus on the ionization of argon at an intensity of $8 \times 10^{13} \text{ W cm}^{-2}$ and at wavelength of 1300 nm. Although the intensity is weaker than those considered above, $\alpha_0 \approx 39$ a.u. here. To achieve such a large value of the excursion amplitude, a 800-nm field should have an intensity of $5.5 \times 10^{14} \text{ W cm}^{-2}$ and a 390-nm field an intensity of $9.8 \times 10^{15} \text{ W cm}^{-2}$. In the same time, the wavelength is still sufficiently short that the photon energy is larger than the binding energy of most of the low-lying dressed excited states and of all the higher-lying ones ($\omega = 0.035$ a.u. at 1300 nm). As far as these dressed states are concerned, and apart for occasional interactions with deeply bound states, the field is thus strong and its frequency is high. We should therefore expect that the excited quasienergy spectrum is similar to that found in the previous section for similarly large values of α_0 . That this is indeed the case can be seen from Fig. 12, which shows how the $(\sigma = 1, m = 0)$ spectrum evolves as the wavelength increases from 800 nm to 1300 nm, the intensity being kept fixed. While

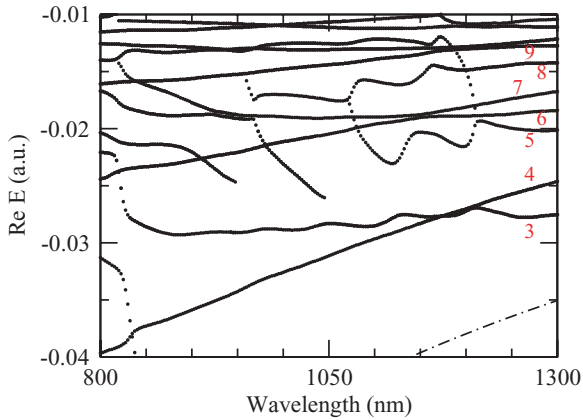


FIG. 12. (Color online) The ($\sigma = 1, m = 0$) quasienergy spectrum of argon at 80 TW cm^{-2} intensity vs. wavelength. No results are shown below the dash-dotted line, which indicates the $\text{Re } E = -\hbar$ threshold. The dressed ground state is not represented.

there are significant difference below 850 nm ($\alpha_0 = 17 \text{ a.u.}$), the structure of the spectrum becomes very similar to that found above 150 TW cm^{-2} in Fig. 6. In particular, most of the large- α_0 states of Fig. 6 are easily identified in Fig. 12. However, States 1 and 2, for which $\text{Re } E < -0.035 \text{ a.u.}$, are absent at 1300 nm .

The dressed excited states the ground state may become resonant with when the intensity varies around 80 TW cm^{-2} are thus large- α_0 states at 1300 nm . As shown by Fig. 13, their crossings with the dressed ground state produce a clear series of resonance enhancements in the total ionization rate. However, these enhancements tend to be significantly

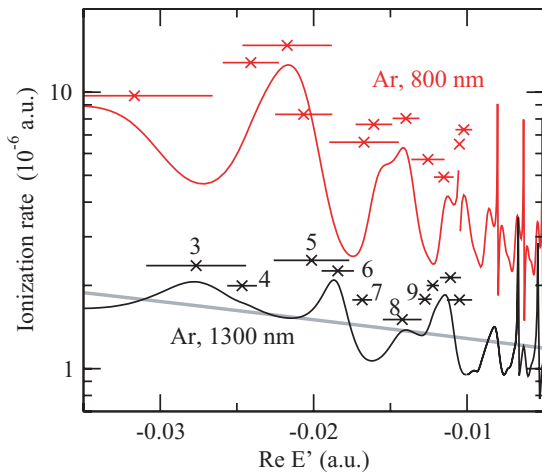


FIG. 13. (Color online) The rate of ionization from the dressed ground state of argon vs. the real part of its quasienergy, at 1300-nm wavelength for intensities between 77 and 81 TW cm^{-2} (lower curve) and at 800-nm wavelength for intensities between 78 and 91 TW cm^{-2} (upper curve). The crosses and horizontal bars (shown only for $\text{Re } E < -0.01 \text{ a.u.}$) indicate the positions of the resonances and the ionization widths of the corresponding dressed excited states at their crossings with the dressed ground state. (Thick gray curve) Ionization rate obtained by summing the ω^2 expansion up to order ω^6 (1300 nm only). The numbers identify the resonant dressed states as per Fig. 12.

weaker than at 800 nm for similar intensities. The overall magnitude of the rate is also smaller, in agreement with Fig. 3. Nonetheless, at both wavelength, avoided crossings with very narrow dressed states give rise to sharp resonance structures close to threshold. The 1300-nm argon results of Fig. 13 are comparable to the 800-nm helium results of Fig. 8(b) in that $\gamma_K \approx 0.79$ in both cases and that the resonant dressed excited states are the same large- α_0 states. The order of the ionization process is similar, too: it takes thirty 1300-nm photons to ionize argon at 80 TW cm^{-2} , and twenty-nine 800-nm photons to ionize helium at 330 TW cm^{-2} . Comparing Fig. 13 to Fig. 8(b), we see that the relative magnitude of the resonance enhancements is similar in both systems, despite the difference in the intensity, and that States 3, 5, and 8 have a larger ionization width than States 4, 6, 7, and 9 both in argon at 1300 nm and in helium at 800 nm .

As found for the other systems studied in this work, we see that the ionization rate of argon at 1300 nm is also correctly predicted by the ω^2 expansion (apart for the resonance structures). On this ground, we expect that the ω^2 expansion is reliable at still longer wavelengths, and therefore that the overall magnitude of the Floquet ionization rate deeper in the infrared is given by the solid curve of Fig. 3 (i.e., Γ_6). Because the basis set required by a Floquet calculation at 80 TW cm^{-2} becomes excessively large, we cannot gauge the importance of the resonances with dressed excited states much above 1300 nm . However, one can expect that they become negligible at much longer wavelengths, since these resonances would normally be with large- α_0 KH states, that the spatial extension of these states increases with α_0 , and therefore that the strength of their coupling with the ground state should vanish in the long wavelength limit.

IV. CONCLUSIONS

In conclusion, we have studied the spectrum of the dressed excited states the ground state may be resonant with when $\gamma_K \ll 1$. We have shown that at wavelengths in the visible or the infrared these dressed excited states are predominantly large- α_0 states akin to the high-frequency KH states supported by the dressed Coulomb potential and that these states undergo strong-field stabilization when the intensity increases. For a given, large value of α_0 , and within the single-active-electron approximation, their spectrum has the same structure for all atoms. For instance, we have shown that the spectrum of the dressed excited states of argon in a field of 1300-nm wavelength and 80 TW cm^{-2} intensity is similar to the spectrum of the dressed excited states of helium in a field of 800-nm wavelength and 500 TW cm^{-2} intensity. Our results indicate that the large- α_0 states group into several series differing by their Stark shift and by their coupling with the dressed ground state.

We have calculated the rate of ionization in a monochromatic laser field for hydrogen and for one-electron models of helium and argon, without making simplifying assumptions on the dynamics of the process. We have found that the importance of the resonances in the ionization from the ground state tends to decrease for increasing values of α_0 . This happens, presumably, because of the concomitant reduction in the spatial overlap of the wave functions of the ground state

and of the resonant dressed excited states. However, interaction with the latter may still affect ionization from the ground state significantly. In particular, we have found that both in hydrogen at 800 nm and in helium at 390 nm the ground state undergoes multiple avoided crossings with excited states at intensities for which $\gamma_K \approx 0.6$, and that their interaction often results in a reduction rather than an enhancement of ionization. A similar reduction is not present in the corresponding time-dependent results of Parker *et al.* [8], although the two calculations are in excellent agreement on the positions of the resonance enhancements. Further work would be desirable to understand the origin of this discrepancy.

Besides the *ab initio* Floquet calculations, we have also obtained the ionization rate within the strong-field approximation, both in its length gauge (Keldysh) formulation and its velocity gauge (Faisal-Reiss) formulation, as well as within the ω^2 -expansion theory of Pont *et al.* [22,23]. For the same model potential, and except where multiphoton resonances are important, these four different approaches all yield total ionization rates in good quantitative agreement with each other

at the intensities and wavelengths considered in this article. The results show that the choice of gauge is not critical in the calculation of the ionization rate in the SFA, in the present context, and they confirm the usefulness of the Coulomb correction proposed by Becker *et al.* [21]. They also indicate that the ω^2 expansion, truncated to its first few terms, gives a good description of the nonadiabatic nature of the tunneling state of ionization in a strong low-frequency laser field.

ACKNOWLEDGMENTS

We thank Jonathan Parker for detailed information on the time-dependent results shown in Fig. 11 and for useful discussions about the comparison between these results and ours. E.M. thanks TÜBİTAK for the support provided for this work under the project 107T308. S.V. is supported by the Ministry of Science and Technological Development of Serbia under the project 141029A. Parts of the calculations presented in this article have been performed on computers financed by the EPSRC.

-
- [1] L. V. Keldysh, Zh. Eksp. Teor. Fiz. **47**, 1945 (1964) [Sov. Phys. JETP **20**, 1307 (1965)].
- [2] W. Becker, F. Grasbon, R. Kopold, D. B. Milošević, G. G. Paulus, and H. Walther, *Adv. At. Mol. Opt. Phys.* **48**, 35 (2002); F. Krausz and M. Ivanov, *Rev. Mod. Phys.* **81**, 163 (2009).
- [3] No resonance structure arising from the coupling of the ground state with intermediate states could have been resolved in the measurements of the ATI spectrum done so far in the tunneling regime, for pulses exceeding 100 fs in duration, because at the high intensities involved they would have been washed out by the focal averaging and the large ponderomotive scattering [see, e.g., B. Walker, B. Sheehy, L. F. DiMauro, P. Agostini, K. J. Schafer, and K. C. Kulander, *Phys. Rev. Lett.* **73**, 1227 (1994)]. Ponderomotive scattering is less severe in ultrafast pulses, but there the short duration of the pulses can be expected to hinder resonance with excited states [see, e.g., G. G. Paulus, F. Grasbon, H. Walther, R. Kopold, and W. Becker, *Phys. Rev. A* **64**, 021401 (2001)].
- [4] The SFA theory has been extended to recollision-free tunnel ionization concomitant with the excitation of the core—see, e.g., W. A. Bryan *et al.*, *Nat. Phys.* **2**, 379 (2006) and references therein. However, here we focus on the process where a singly excited state of the original atom acts as an intermediate state in the detachment of the valence electron.
- [5] R. R. Freeman, P. H. Bucksbaum, H. Milchberg, S. Darack, D. Schumacher, and M. E. Geusic, *Phys. Rev. Lett.* **59**, 1092 (1987).
- [6] R. M. Potvliege and R. Shakeshaft, *Phys. Rev. A* **40**, 3061 (1989).
- [7] R. Shakeshaft, R. M. Potvliege, M. Dörr, and W. E. Cooke, *Phys. Rev. A* **42**, 1656 (1990).
- [8] J. S. Parker, K. J. Meharg, G. A. McKenna, and K. T. Taylor, *J. Phys. B* **40**, 1729 (2007).
- [9] J. S. Parker, G. S. J. Armstrong, M. Boca, and K. T. Taylor, *J. Phys. B* **42**, 134011 (2009).
- [10] H. G. Muller, *Phys. Rev. Lett.* **83**, 3158 (1999).
- [11] H. G. Muller, *Opt. Express* **8**, 86 (2000).
- [12] M. Gavrilu, *Adv. At. Mol. Opt. Phys. Suppl.* **1**, 435 (1992).
- [13] M. Pont, N. R. Walet, and M. Gavrilu, *Phys. Rev. A* **41**, 477 (1990).
- [14] E. Meşe and R. M. Potvliege, *Phys. Rev. A* **77**, 023414 (2008).
- [15] A. Maquet, Shih-I. Chu, and W. P. Reinhardt, *Phys. Rev. A* **27**, 2946 (1983); S. Graffi, V. Grecchi, and H. J. Silverstone, *Ann. Inst. Henri Poincaré Phys. Théor.* **42**, 215 (1985), and references therein.
- [16] R. M. Potvliege and R. Shakeshaft, *Adv. At. Mol. Opt. Phys. Suppl.* **1**, 373 (1992); S.-I. Chu and D. A. Telnov, *Phys. Rep.* **390**, 1 (2004).
- [17] A. M. Perelomov, V. S. Popov, and M. V. Terent'ev, Zh. Eksp. Teor. Fiz. **50**, 1393 (1966) [Sov. Phys. JETP **23**, 924 (1966)].
- [18] A. M. Perelomov and V. S. Popov, Zh. Eksp. Teor. Fiz. **52**, 514 (1967) [Sov. Phys. JETP **25**, 336 (1967)].
- [19] F. H. M. Faisal, *J. Phys. B* **6**, L89 (1973).
- [20] H. R. Reiss, *Phys. Rev. A* **22**, 1786 (1980).
- [21] A. Becker, L. Plaja, P. Moreno, M. Nurhuda, and F. H. M. Faisal, *Phys. Rev. A* **64**, 023408 (2001); See also A. Becker and F. H. M. Faisal, *ibid.* **59**, R1742 (1999); The validity of this Coulomb correction has been discussed by H. R. Reiss [*ibid.* **65**, 055405 (2002)] and by C. C. Chirilă [Ph.D. thesis (University of Durham, 2004)].
- [22] M. Pont, R. Shakeshaft, and R. M. Potvliege, *Phys. Rev. A* **42**, 6969 (1990).
- [23] M. Pont, R. M. Potvliege, R. Shakeshaft, and Z.-j. Teng, *Phys. Rev. A* **45**, 8235 (1992).
- [24] R. M. Potvliege and S. Vučić, *Phys. Rev. A* **74**, 023412 (2006).
- [25] R. M. Potvliege, *Comput. Phys. Commun.* **114**, 42 (1998). The FORTRAN code is distributed by the Computer Physics Communications Program Library.
- [26] M. J. Nandor, M. A. Walker, L. D. Van Woerkom, and H. G. Muller, *Phys. Rev. A* **60**, R1771 (1999).
- [27] V. S. Popov, *Usp. Fiz. Nauk* **174**, 921 (2004) [*Phys. Usp.* **47**, 855 (2004)].

- [28] N. B. Delone and V. P. Krainov, *Multiphoton Processes in Atoms* (Springer, Berlin, 1994).
- [29] B. M. Smirnov and M. I. Chibisov, *Zh. Eksp. Teor. Fiz.* **49**, 841 (1965) [*Sov. Phys. JETP* **22**, 585 (1966)].
- [30] In Ref. [21], Becker *et al.*, multiply the single-active-electron rate by a factor of 2 to account for the presence of two equivalent electrons in the ionizing shell. For consistency with the other methods considered in this article, we do not make this correction.
- [31] C. Leubner, *Phys. Rev. A* **23**, 2877 (1981).
- [32] The variation of the momentum-space wave function of the initial state has been shown to modulate the ATI spectrum at low frequencies [H. R. Reiss, *Phys. Rev. Lett.* **102**, 143003 (2009)]. This variation plays no role in the oscillations of the total ionization rate discussed here.
- [33] The convergence to the adiabatic rate at increasing intensities and wavelengths has already been illustrated in Refs. [7,22,23] and, more recently, Ref. [9].
- [34] P. Colosimo *et al.*, *Nat. Phys.* **4**, 386 (2008).
- [35] R. J. Vos and M. Gavrilu, *Phys. Rev. Lett.* **68**, 170 (1992); R. M. Potvliege and P. H. G. Smith, in *Super Intense Laser-Atom Physics*, edited by B. Piraux, A. L'Huillier, and K. Rzażewski (Plenum Press, New York, 1993), p. 173.